

GAP-LA: GPU-Accelerated Performance-Driven Layer Assignment

Chunyuan Zhao, Zizheng Guo, Zuodong Zhang, Yibo Lin, *Member, IEEE*

Abstract—Layer assignment is critical for global routing of VLSI circuits. It converts 2D routing paths into 3D routing solutions by determining the proper metal layer for each routing segments to minimize congestion and via count. As different layers have different unit resistance and capacitance, layer assignment also has significant impacts to timing and power. With growing design complexity, it becomes increasingly challenging to simultaneously optimize timing, power, and congestion efficiently. Existing studies are mostly limited to a subset of objectives. In this paper, we propose a GPU-accelerated performance-driven layer assignment framework, GAP-LA, for holistic optimization the aforementioned objectives. Experimental results demonstrate that we can achieve 0.3%-9.9% better worst negative slack (WNS) and 2.0%-5.4% better total negative slack (TNS) while maintaining power and congestion with competitive runtime compared with ISPD 2025 contest winners, especially on designs with up to 12 millions of nets

Index Terms—Physical design, Global routing, Layer assignment, Timing, Power, GPU acceleration.

I. INTRODUCTION

Global routing is an important step in modern very-large-scale-integrated (VLSI) physical design flow. It partitions the layout into a set of GCells and finds a GCell-level routing solution of each signal net. The solution serves as early routing planning for the detailed routing stage and offers fast metric feedback such as congestion for the placement stage. Figure 1 presents a typical 2D global routing flow, which can be divided into 2 phases: 2D routing and layer assignment. 2D routing decides the connections between components while optimizing wirelength and congestion by projecting 3D routing resources into a 2D resource model. After that, layer assignment is invoked to assign those 2D routing segments to proper layers to generate the expected 3D global routing solution while minimizing congestion and via count.

To achieve better design performance, layer assignment needs to optimize for timing and power instead of those indirect metrics. Timing is determined by cell delay and net delay, which are highly correlated to the parasitic resistance and capacitance of nets. Power is correlated to the parasitic capacitance of nets. As unit resistance and capacitance of low metal layers can be several times larger than high metal layers, layer assignment can have significant impacts to timing and power.

Prior works on layer assignment can be roughly categorized into congestion-driven and delay-driven approaches. Congestion-driven layer assignment focuses on net ordering, escaping local optima strategies and refinement process to minimizing congestion. Lee and Wang [1] design net ordering strategy considering net wirelength, number of pins and average density. They also apply a dynamic programming method

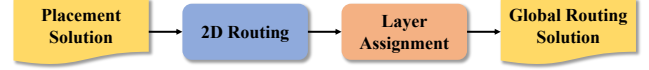


Fig. 1. Typical 2D global routing flow [4].

and an examination method to avoid violating congestion constraints. In [2], they take via capacity proposed by [3] and bending point cost into account for a better congestion in more accurate resource model. FastRoute [4] further introduces an edge order strategy in layer assignment process. [5], [6] use negotiation-based method to penalize congestion region to escape local optima and [6] introduces layer shifting method to refine after rip-up and re-assign process. To avoid solution space being restricted by net ordering, COALA [7] assigns wires concurrently. [8]–[11] integrate layer assignment into 2D routing to optimize congestion in 3D resource model directly.

Delay-driven layer assignment focuses on minimizing maximal or average delay of routing segments under congestion constraints. [12], [13] prioritize nets with large delay and formulate the delay optimization problem as an ILP problem. [14]–[16] take coupling effect, slew and non-default-rule routing into account to better handle delay optimization problem in advanced technology node. They also apply edge weighting strategy to optimize maximal and average delay of sinks effectively. It usually takes around ten minutes for those CPU layer assignment frameworks to handle the design with around ten million pins and one million GCells.

However, the aforementioned methods still face challenges, such as insufficient runtime efficiency in modern large-scale designs and the neglect of direct optimization of timing metrics like TNS and WNS. To optimize TNS and WNS, layer assignment is desired to have a comprehensive analysis across the entire circuit design and introduce effective optimization strategy instead of only considering maximal and average delay. As design complexity and scale grows, layer assignment on CPU is facing runtime efficiency problem. In recent years, GPU acceleration techniques have demonstrated significant potential in physical design (PD). Leveraging the massive parallel computing power of GPUs, the runtime of many traditional problems has been reduced by tens of times, particularly in the placement [17]–[22] and routing [9], [10], [23]–[25] stages. However, very few research has explored efficient optimization of timing and power in layer assignment with GPU acceleration.

To tackle the performance optimization of such challenging cases, we propose GAP-LA, which utilizes different strategies and GPU-accelerated layer assignment kernels to achieve high-quality 3D global routing solution.

We summarize our main contributions as follows:

- We present a performance-driven layer assignment frame-

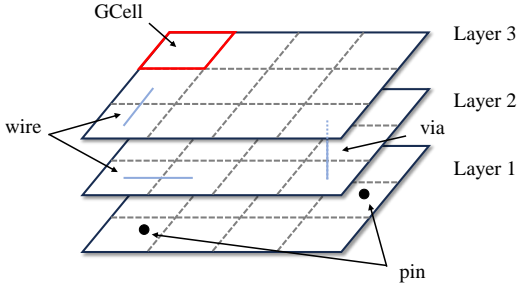


Fig. 2. GCell grid graph in global routing.

work GAP-LA with GPU acceleration. In this framework, we consider net delay and net capacitance to optimize timing and power.

- We propose a net ordering strategy considering timing information reported by static timing analysis to prioritize the timing critical nets for explicit WNS and TNS optimization effectively.
- We propose a look ahead strategy to handle delay cost in tree dynamic programming-based layer assignment method and fully accelerate the assignment process with GPU.

Experimental results show that, compared with the top-3 winners in ISPD25 Contest [26], our method achieve 0.3%-9.9% better WNS and 2.0%-5.4% better TNS while maintaining comparable power consumption and congestion.

The rest of the paper is organized as follows. Section II introduces the background of our performance-driven layer assignment algorithms and the problem formulation. Section III explains our strategies and GPU kernels used in GAP-LA. Section IV validates our approach with comprehensive experimental results. Section V concludes our paper.

II. PRELIMINARIES

A. GCell in Global Routing

In the modern physical design flow, as demonstrated in Figure 2, the 3D multi-layer design is partitioned into small rectangular units called GCells by (usually evenly spaced) horizontal and vertical grid lines. To align with the actual manufacture, routing segments are constrained to this grid graph and each edge is assigned a capacity value to characterize its available routing resource. We denote the edge between two GCells on the same layer wire and the edge between two GCells on the adjacent layers via. In a traditional global routing flow, the router finds a 2D solution and then applies layer assignment to get a well optimized 3D solution.

B. Layer Assignment

Layer assignment typically takes a GCell grid graph with GCell edge capacity, a netlist and an optimized 2D global routing solution as input and assigns each 2D routing segment to a certain layer to generate a 3D global routing solution. As illustrated in Figure 3a and Figure 3b, the layer assignment process successfully derives a 3D solution. Notably, this newly obtained 3D solution maintains the exact same projection as

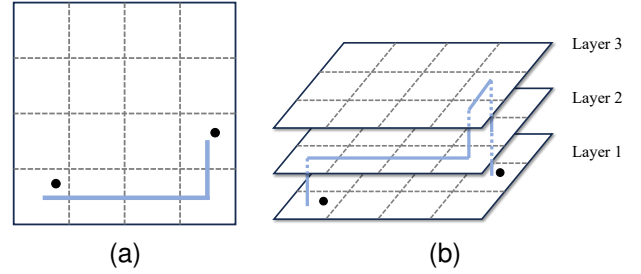


Fig. 3. (a) 2D global routing solution for a net. (b) 3D global routing solution after layer assignment process.

the input 2D solution. A typical layer assignment flow reorders the input nets and performs tree dynamic programming kernel to optimize each net in sequential order. The common objective is usually weighted sum of total overflow and via count. In performance-driven layer assignment problem, the objective also involves worst negative slack (WNS), total negative slack (TNS) and power consumption, which are reported by static timing analysis and power analysis tool.

C. Static Timing Analysis

Static timing analysis (STA) is an essential step to ensure the performance of the design during the physical design flow. It represents the circuit as a directed acyclic graphs (DAG), where nodes denote pins of circuit components and edges denote pin interconnects. A typical STA engine performs timing propagation to obtain arrival time, required arrival time, slack, and eventually critical paths. After these two steps, slack of pins, critical paths and other timing information are reported. The slack of a pin is the difference between its required arrival time and arrival time and describes the extent of timing violation of the pin. The critical path of a primary output leads to the longest delay and worst slack from primary input to it. Many different kinds of delay models can be used by an STA engine. In our framework, we compute cell delays through the nonlinear delay model (NLDM) based on 2D lookup tables with load and slew indices and Elmore delay model [27] is applied to get net delay. These models are widely used in recent academic research and contests.

D. Problem Formulation

Given a layout partitioned into rectangular subregions (GCells) by a set of horizontal and vertical grid lines, and a GCell-level 2D routing solution for nets, performance-driven layer assignment determines a 3D routing solution for each net. The process simultaneously optimizes WNS, TNS, power consumption, and total overflow. Critically, the planar projection of the 3D result must strictly match the input 2D solution.

E. Evaluation Metrics

In this work, we follow the same evaluation method as the ISPD25 Performance-driven Large Scale Global Routing Contest [26], which is defined as follows:

Quality score: Quality score is defined by the weighted sum of WNS, TNS, power consumption and total overflow,

$$w_1 \cdot (WNS - r_1) + w_2 \cdot \frac{TNS - r_2}{N_{end}} + w_3 \cdot (pow - r_3) + w_4 \cdot tof, \quad (1)$$

where w_1, w_2, w_3, w_4 are input for each design to adjust the weights of different metrics and r_1, r_2, r_3 are input reference metric value. N_{end} is the number of end points in the design and tof is total overflow of all the GCell edges. In our evaluation flow, WNS, TNS and $power$ are reported by open source tool OpenROAD [28]. Note that, value of r_1, r_2, r_3 does not influence the comparison among different solutions because value of $w_1 \cdot r_1, w_2 \cdot r_2, w_3 \cdot r_3$ is constant. Table I lists the detailed information of 12 cases in ISPD2025 contest.

Overflow: For a GCell edge e on layer l , its overflow is usually computed with its demand d and capacity c in previous works as follows,

$$of = \max\{0, d - c\}. \quad (2)$$

To align with ISPD25 Contest evaluation metrics [26], we use

$$of = ofw(l) \cdot e^{s(d-c)} \quad (3)$$

as its overflow, where s is 0.5 for $c > 0$, 1.5 for $c = 0$, and $ofw(l)$ denotes the overflow weight of layer l , which is given in the benchmark.

III. ALGORITHMS

Figure 4 illustrates the overall framework of GAP-LA, which takes a netlist, routing graph, and 2D global routing solution as inputs and ultimately generates a well-optimized 3D global routing solution. After loading the netlist, global routing graph, and 2D solution data, we conduct a static timing analysis on the GPU using HeteroSTA [29]–[31]. Leveraging the timing report, we identify critical nets and prioritize their assignment. Guided by net criticality insights, we carefully implement net ordering to enhance both performance and overflow outcomes. Next, we generate multiple net batches based on this ordering and perform parallel layer assignment for nets within the same batch on the GPU. Finally, our framework yields a 3D global routing solution with optimized performance metrics.

A. Critical Net Analysis-based Net Ordering and Batching Strategy

The delay of critical paths is of paramount importance for design timing closure, and our solution aims to minimize

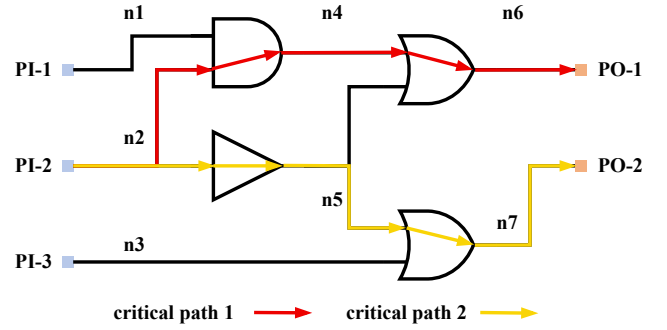


Fig. 5. An example of critical paths in the static timing analysis graph.

critical path delay as much as possible. However, since layer assignment is a net-based optimization operation, the delay of critical paths cannot be optimized directly. Therefore, identifying the criticality of each net is essential.

Figure 5 depicts an example of a static timing analysis graph with three primary inputs and two primary outputs. The static timing analysis engine reports one critical path for each primary output: Critical path 1 traverses nets n_2, n_4 , and n_6 while critical path 2 traverses nets n_2, n_5 , and n_7 . We define net criticality as the number of critical paths traversing the net. In example shown in Figure 5, net n_2 exhibits the highest criticality, whereas nets n_4, n_5, n_6 and n_7 have lower criticality, and all other nets have the lowest criticality. Intuitively, optimizing a net with higher criticality yields greater benefits, as it may dominate the arrival times of multiple primary outputs.

In a typical sequential layer assignment flow, net ordering is a crucial determinant of the final routing solution quality. We prioritize the critical nets identified earlier, as they exert the most significant impact on the arrival times of primary outputs. In our flow, the static timing analysis engine reports the top-1 worst critical paths of every primary output with slack worse than $0.7 \times WNS$. Nets traversed by more than three relevant critical paths are designated as critical nets. For each net, we define its net slack as the minimum slack value among its pins. After processing these critical nets, nets with critical net slack (worse than $0.7 \times WNS$) become critical, as low slack indicates they may dominate critical paths if the delay of original critical paths is reduced by assigning relevant nets to upper layers. We call these nets semi-critical nets. As an illustrated in Figure 5, after optimizing critical nets n_2, n_4, n_5, n_6 and n_7 , net n_3 may dominate the arrival time of PO-2, so that it should be prioritized. Layer assignment for the remaining nets follows subsequently.

However, the strategy described above is purely sequential and must be adapted for parallel computing. Our observations indicate that nets with similar criticality and slack have comparable impacts on final design performance. As a result, strict net ordering can be relaxed: we partition the net set into multiple subsets, enabling parallel assignment within each subset with minimal quality degradation. For critical and semi-critical nets, let C denote the maximum criticality. We place nets with criticality $[C, C]$ into the first subset, $[\frac{C}{2}, C)$ into the second subsets, $[\frac{C}{4}, \frac{C}{2})$ into the third subsets and so

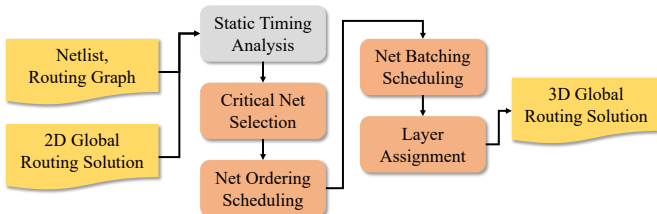


Fig. 4. The overall framework of GAP-LA.

Algorithm 1 Critical Net Analysis-based Net Ordering and Batching Strategy.

Input: netlist N , 2D routing solution $GRS-2D$, average resistance of unit length metal r_{avg} , average capacitance of unit length metal c_{avg} , static timing analysis engine STA, semi-critical slack ratio α , threshold th

Output: Batches BS

- 1: $pin_slack, crit_paths \leftarrow STA(GRS-2D, r_{avg}, c_{avg}, \alpha)$
 - 2: $criticality \leftarrow Count(N, crit_paths)$
 - 3: $N_c, N_s, N_n \leftarrow Divide(N, criticality, pin_slack, th)$
 - 4: $S_c \leftarrow PartitionAndSort(N_c)$
 - 5: $S_s \leftarrow PartitionAndSort(N_s)$
 - 6: $S_n \leftarrow Sort(N_n)$
 - 7: $BS_c \leftarrow GetBatches(S_c)$
 - 8: $BS_s \leftarrow GetBatches(S_s)$
 - 9: $BS_n \leftarrow GetBatches(S_n)$
 - 10: $BS \leftarrow Concat(BS_c, BS_s, BS_n)$
-

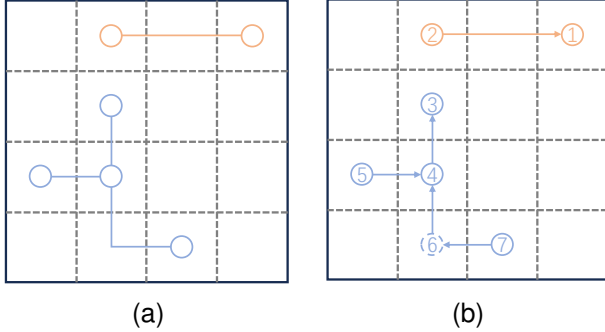


Fig. 6. (a) The original 2D routing structure. Net 1 has 2 nodes and net 2 has 4 nodes. (b) Our layer assignment directed tree. Net 1 has 2 nodes and net 2 has 5 nodes.

on. For other nets with bad slack, we place nets with slack $[WNS, WNS]$ into the first subset, $[0.99 \cdot WNS, WNS]$ into the second subset, $[0.96 \cdot WNS, 0.99 \cdot WNS]$ into the third subset and so on. For non-critical nets (better than $0.7 \times WNS$), we employ a traditional congestion-driven strategy instead, as these nets are far less likely to degrade design performance. Algorithm 1 outlines our critical net analysis-based net ordering and batching strategy flow.

B. Layer Assignment Directed Tree

To facilitate the extraction of parasitic parameters and the implementation of a fine-grained parallel layer assignment algorithm, we designed a directed tree structure. In our layer assignment algorithm, we assume that a straight 2D routing segment should be assigned to a single layer without layer shifting, which is only performed at bends and Steiner points. To satisfy these constraints, we introduce additional nodes to ensure all inter-node connections are strictly straight, so layer shifting operations are confined to nodes in the directed tree. As illustrated in Figure 6a and Figure 6b, node 6 is added to bridge node 4 and node 7, ensuring no routing paths with bend points exist in the directed tree.

Based on the tree discussed above, we extract parasitic parameters for static timing analysis. The directed tree acts as a subgraph in the STA graph, with nodes connected to relevant pin nodes in the STA graph via zero-resistance edges. For horizontal (vertical) wire connections, we calculate resistance (capacitance) using the average per-unit-length resistance (capacitance) of all horizontal (vertical) wires. We then compute the resistance of all edges and capacitance of all nodes in the STA graph using the widely adopted π -model.

C. Directed Tree Edge Weighting

Due to the fact that each net has distinct criticality, our algorithm allocates varying optimization efforts to reduce the delay and capacitance of different nets. In prior studies such as [20], net weighting has emerged as a prevalent approach to tackle this challenge. However, this approach overlooks the fact that each sink of a net has distinct criticality. As demonstrated in Figure 7a, sink 1 has estimated slack of -1 ps and sink 2 has estimated slack of -100 ps. Since sink 2 exhibits a significantly worse negative slack than sink 1, optimizing the delay from the net source to sink 2 warrants greater effort. Figure 7b illustrates that the pin weight follows a logistic function of $\frac{slack}{WNS}$:

$$w_{pin} = \frac{1}{1 + k \left(\frac{slack}{WNS} - b \right)}, \quad (4)$$

and we select $k = 10, b = 0.3$ in our implementation. The logistic function value remains nearly 1 as $\frac{slack}{WNS}$ approaches 1, enabling our algorithm to effectively optimize paths with poor slack. For an edge in the directed tree, its weight is defined as the maximum weight of all sinks in its downstream subtree:

$$w_{e:u \rightarrow v} = \max_{pin \in subtree(u)} w_{pin} \quad (5)$$

D. Layer Assignment with Look Ahead Strategy

To concurrently optimize slack, power consumption, and congestion, we integrate three cost functions: net delay cost, net capacitance cost, and net congestion cost. Net capacitance is prioritized here, as it directly influences both power consumption and cell delay. In the Nangate 45nm library, cell delay dominates path delay: a cell may exhibit equivalent

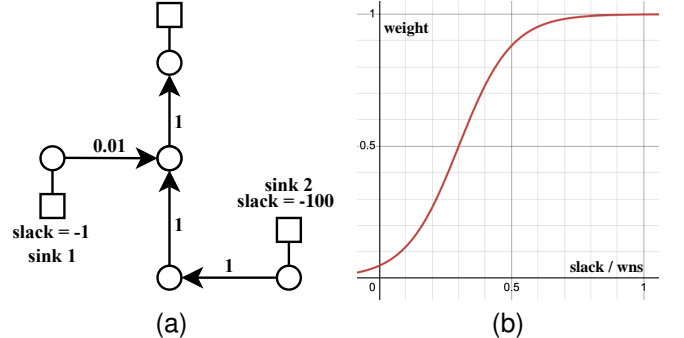


Fig. 7. (a) Direct tree edge weighting. (b) Pin weight is the logistic function of its $\frac{slack}{WNS}$.

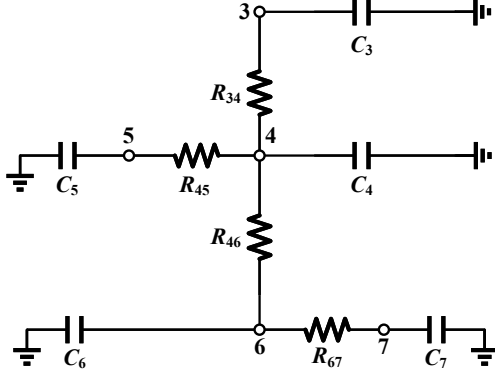


Fig. 8. RC tree of net 2 in Figure 6b.

Algorithm 2 Layer Assignment

Input: delay/capacitance/congestion weight w^d , w^{cap} and w^{cong} , batches BS , node son/parent node/pin list $sons, par, pin$, node position x, y , resistance (R) and capacitance (C) of unit length on each layer r, c , R of via on each layer vr , estimated upstream R of each node ur , downstream load C of candidate solution dlc , the lowest layer with pin of a node nl , the highest layer with pin of a node nh , layout size X, Y, L , demand map D and capacity map C

Output: 3D routing solution $GRS-3D$

```

1: for batch in BS do
2:   for level = 0 to max level of batch do
3:     Call getSubtreeCandidate
4:   end for
5:   for level = max level of batch to 0 do
6:     Call traceBackSolution
7:   end for
8: end for

```

drive resistances exceeding $1k\Omega$, whereas the resistance of a GCell edge remains below $0.01k\Omega$. In a typical congestion- and via count-driven sequential layer assignment framework, we employ tree dynamic programming (DP) to optimize the objective for each net. The tree DP method proceeds bottom-up to compute the optimal solution for each candidate subtree, then top-down to backtrack the optimal solution for the entire tree. For each node, DP retains the optimal solution for each possible layer through which the path from the node to its

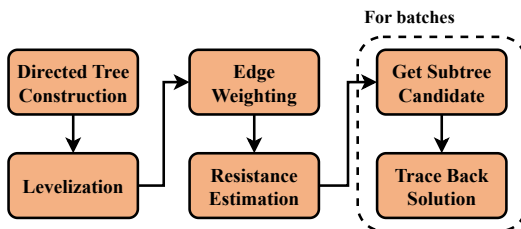


Fig. 9. Layer assignment flow.

Algorithm 3 Get Subtree Candidate

Input: level to get candidate

Output: candidate solution cost f , candidate solution look ahead cost f' , candidate solution layer selection entry

```

1:  $idx \leftarrow \text{threadIdx.x} + \text{blockDim.x} \times \text{blockIdx.x}$ 
2:  $n \leftarrow \text{GetLevelNode}(\text{level}, \lfloor \frac{idx}{L} \rfloor)$ 
3:  $l \leftarrow idx - n \times L$  ▷ node  $n$ , layer  $l$ 
4:  $f_{n,l} \leftarrow 0, dlc_{n,l} \leftarrow 0$ 
5: for  $pin \in pins_n$  do
6:    $d \leftarrow pin_{cap} \cdot vr(pin_l \rightarrow l)$ 
7:    $f_{n,l} \leftarrow f_{n,l} + d \cdot w_{n \rightarrow par_n}^d, dlc_{n,l} \leftarrow dlc_{n,l} + pin_{cap}$ 
8: end for
9: for  $b = 0$  to  $L - 1$  do
10:  if  $b > nl$  or  $b > l$  then
11:    continue
12:  end if
13:   $vcong \leftarrow 0$ 
14:  for  $t = b$  to  $L - 1$  do
15:     $g_{n,b,t} \leftarrow 0, g'_{n,b,t} \leftarrow 0, cap_{n,b,t} \leftarrow 0$ 
16:     $vcong \leftarrow vcong + \text{ViaCong}(x_n, y_n, t, D, C)$ 
17:    if  $t \geq nh$  and  $t \geq l$  then
18:      for  $son$  in  $sons_n$  do
19:        for  $son\_l = b$  to  $t$  do
20:           $cost_{son,son\_l} \leftarrow f_{son,son\_l} + dcost + ccost + wccost$ 
21:           $cost'_{son,son\_l} \leftarrow cost_{son,son\_l} + w_{son \rightarrow n}^d \cdot ur_n \cdot (dlc_{son,son\_l} + wcap)$ 
22:        end for
23:         $best_{son,b,t} \leftarrow \arg \min_{i \in [b,t]} cost'_{son,i}$ 
24:        Update  $cap_{n,b,t}, g_{n,b,t}, g'_{n,b,t}$  to record cost and load capacitance.
25:      end for
26:    end if
27:  end for
28:   $choice_{n,l} \leftarrow \arg \min_{(b,t)} g'_{n,b,t}$ 
29:   $f_{n,l} \leftarrow f_{n,l} + g_{n,choice_{n,l}}, dlc_{n,l} \leftarrow dlc_{n,l} + cap_{n,choice_{n,l}}$ 
30:  for  $son$  in  $sons_n$  do
31:     $entry_{n,l,son} \leftarrow best_{son,b,t}$ 
32:  end for

```

parent traverses. However, this method is ineffective for net delay optimization due to the after-effect. Figure 8 shows the RC tree extracted from net 2 in Figure 6b using the π -model, where node 3 is the root of the tree and node 5, 6, 7 are the leaves. In the Elmore delay model, the delay from node 3 to node 4 d_{34} is computed as $R_{34} \times (C_4 + C_5 + C_6 + C_7)$. The subtree choices for nodes 5, 6, and 7 introduce after-effects on d_{34} , which is absent in congestion or wirelength cost calculations. Due to the significant resistance of vias, routing a simple 2-pin net on lower layers reduces net delay but increases net capacitance. As a result, small subtrees tend to favor lower layers for reduced delay, which can degrade the delay of upstream connections. To address this, we propose a look-ahead strategy. Let f_u denote the cost of the subtree rooted at node u comprising delay, capacitance, and congestion costs. In our layer assignment directed tree, we estimate the upstream

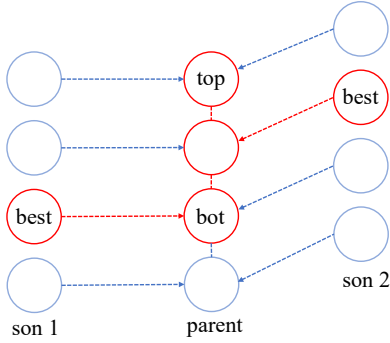


Fig. 10. Enumerate possible son candidates and via connection in Algorithm `getSubtreeCandidate`.

resistance of each node and use $f'_u = f_u + w^d \times r_u^{est} \times c_u$ to select optimal candidate instead of f_u , where w^d is the weight of delay cost, r_u^{est} is the estimated upstream resistance of node u and c_u is the downstream capacitance of node u . This approach anticipates after-effects by evaluating how downstream capacitance contributes to the entire tree's delay cost. For example in Figure 6b and 8, we first estimate resistances R_{34}^{est} , R_{45}^{est} , R_{46}^{est} and R_{67}^{est} using node distances and the average unit-length metal resistance r_{avg} . We then use $f'_6 = w^{cong} \times cong_{67} + w^{cap} \times c_{67} + w^d \times (d_{67} + r_{67}^{est} \times c_6)$ to evaluate all the candidates solution for subtree 6. Figure 9 illustrates our layer assignment flow. After the preparation steps, we obtain the directed tree structure, level information, weighting of each edge, and resistance values for the look-ahead strategy. The algorithm then proceeds to the most computation-intensive part in Algorithm 2.

Algorithm 3 details our GPU kernel implementation. Each GPU thread computes the cost $f_{n,l}$ and look-ahead cost $f'_{n,l}$ of node n at layer l . The implementation first calculates the via delay cost for each pin at the node (Lines 4–7), then enumerates all possible via connection pairs (b, t) (connect layer b to layer t) used at node n and its son nodes (Lines 9–26). For each son node, the candidate subtree with the minimum look-ahead cost is selected, and finally the cost, corresponding solution, and downstream load capacitance are

Algorithm 4 Trace Back Solution

Input: cost list f , choice list $choice$, $level$ to trace back

Output: 3D routing solution $GRS-3D$

```

1:  $idx \leftarrow \text{threadIdx.x} + \text{blockDim.x} \times \text{blockIdx.x}$ 
2:  $n \leftarrow \text{GetLevelNode}(level, idx)$ 
3: if  $n$  is root node then
4:    $best_n \leftarrow \arg \min_{l \in \{0,1,\dots,L-1\}} f_{n,l}$ 
5: end if
6:  $b, t \leftarrow choice_{n,best}$ 
7: Add via  $(x_n, y_n, b) - (x_n, y_n, t)$  to  $GRS-3D$ 
8: for son in  $sons_n$  do
9:    $best_{son} \leftarrow \text{entry}_{n,best_n,son}$ 
10:  Add wire  $(x_n, y_n, best_{son}) - (x_{son}, y_{son}, best_{son})$  to  $GRS-3D$ 
11: end for

```

recorded. Fig. 10 shows the enumeration process at the parent node, where a via connection from layer bot to top is used and son nodes must connect by wires on these layers. The optimal legal candidate with minimal look-ahead cost is chosen for each son.

Algorithm 4 obtains the 3D routing solution from the candidate subtrees computed in Algorithm 3. The root node solution with minimal total cost is selected, and the corresponding subtree solutions for its sons are backtracked. Though conceptually recursive, the implementation uses a GPU-friendly BFS process.

IV. EXPERIMENTAL RESULTS

We implemented our GPU-accelerated layer assignment algorithm using C++ and CUDA on top of HeLEM-GR [25] and HeteroSTA [29]–[31], and evaluated the results on benchmarks from the ISPD25 contest [26] released by NVIDIA. The ISPD25 contest released 12 industrial designs synthesized with the Nangate 45nm open library technology node and specified an official evaluation flow to assess routing solution performance, as detailed in II. All experiments were conducted on a Linux server equipped with a 32-core Intel Xeon Gold CPU@2.90GHz and an NVIDIA A100 GPU. To match the contest evaluation setup, we used the official evaluator for overflow assessment and OpenROAD for evaluating TNS, WNS, and power consumption.

A. Main Comparison with Top-3 Winners in the Contest

We obtained the top-3 contest winners' results and reproduced their experiments on our hardware for comparison. Table II presents a comparison of quality scores and runtime against the ISPD 2025 contest's top-3 winners. Our framework achieved the highest quality score in 9 out of 12 benchmark cases, with comparable performance in the remaining 3 cases. While our static timing analysis engine incurs a 25% runtime overhead due to parsing netlist (.v) and Synopsys design constraints (.sdc) files, the optimization method remains efficient and effective—demonstrating competitive performance relative to the top-3 winners.

Table III presents the WNS, TNS, power consumption, and congestion results of four routers across 12 benchmark cases. The 2nd-place winner produces solutions with favorable performance and low congestion, while the 3rd-place winner demonstrates better performance at the expense of higher congestion. The 1st-place winner achieves a more balanced trade-off among metrics [26]. Our method delivers superior performance with acceptable congestion increase, which can be attributed to the critical net analysis-based net ordering and batching strategy. As shown in Table III, compared to the 1st-place winner, our router achieves 9.9% better WNS, 4.5% better TNS, 1.1% lower power consumption, and 3.8% higher congestion. Versus the 2nd-place winner, we achieve 0.3% better WNS, 5.4% better TNS, 1.5% lower power consumption, and 15.5% higher congestion. In contrast, the 3rd-place winner shows only 0.4% lower power consumption but suffers 4.4% worse WNS, 2.0% worse TNS, and 35.2% higher congestion compared to our approach.

TABLE I
BENCHMARK DETAILS.

Case [†]	Name	$w_1/w_2/w_3/w_4$	$r_1/r_2/r_3$	N_{end}	N_{net}	GCell Graph Dimensions
1	ariane_v	10 / 100 / 300 / 3e-6	-0.485 / -1398.39 / 0.646	20218	123900	10×761×761
2	bsg_v	-10 / -100 / 25 / 4e-8	-0.44 / -10802.7 / 3.05	214821	736883	10×1384×1384
3	nvdla_v	-0.05 / -0.5 / 25 / 1.5e-7	-94.78 / -669471 / 2.96	45925	199481	10×1120×1120
4	tile_v	-1 / -10 / 300 / 7e-7	-0.695 / -3590.83 / 0.1455	13350	136120	10×428×428
5	group_v	-1 / -10 / 20 / 3e-8	-0.815 / -41740.2 / 7.82	347869	3274611	10×1611×1610
6	cluster_v	-1 / -10 / 0.3 / 5e-9	-0.68 / -79748 / 23.7	1082397	12047279	10×3175×3175
7	ariane_b	-0.2 / -2 / 100 / 4e-7	-1.628 / -523.038 / 0.156	20218	105924	10×646×646
8	bsg_b	-0.1 / -1 / 50 / 2e-8	0 / 0 / 0.305	214915	768239	10×1384×1384
9	nvdla_b	-0.01 / -0.1 / 100 / 1e-7	0 / 0 / 0.136	45925	157744	10×1120×1120
10	tile_b	-3 / -30 / 100 / 1e-6	-0.483 / -1920.724 / 0.145	13350	135814	10×386×386
11	group_b	-0.5 / -5 / 3 / 4e-8	-0.68 / -40487.883 / 8.547	347869	3218496	10×1611×1610
12	cluster_b	-0.4 / -4 / 2 / 1e-8	-0.29 / -53249 / 24.261	1082397	12168735	10×3719×3719

[†] *_v and *_b denote the visible and blind cases in the contest, respectively.

TABLE II
COMPARISON OF QUALITY SCORE AND RUNTIME WITH TOP-3 WINNERS IN THE ISPD 2025 CONTEST.

Case	Quality Score							Runtime (s)				
	1st	Imp.	2nd	Imp.	3rd	Imp.	Ours	1st	2nd	3rd	Ours [†]	GAP [‡]
1	0.896	-2.055	0.639	-1.797	0.094	-1.253	-1.158	5	6	14	9	4
2	0.562	-0.640	0.722	-0.800	0.094	-0.172	-0.078	22	16	32	29	9
3	-1.995	-0.137	-2.077	-0.055	-1.824	-0.308	-2.132	7	6	17	12	6
4	-0.405	+0.072	0.401	-0.734	1.370	-1.703	-0.333	7	8	15	8	4
5	-2.029	-1.671	-1.295	-2.406	-3.599	-0.101	-3.700	98	111	197	117	43
6	0.510	-0.135	0.399	-0.024	0.714	-0.339	0.375	330	454	792	513	88
7	1.792	-0.267	1.659	-0.133	1.531	-0.005	1.525	6	6	18	9	4
8	0.849	-0.409	0.415	+0.026	0.689	-0.248	0.441	25	16	38	32	13
9	1.431	-0.077	1.661	-0.307	1.392	-0.038	1.354	6	9	15	8	5
10	0.344	-0.122	2.074	-1.853	1.803	-1.582	0.221	6	9	15	8	3
11	1.332	-0.000	1.232	+0.099	3.116	-1.784	1.331	98	110	200	123	43
12	2.327	-0.500	2.370	-0.544	2.677	-0.851	1.826	351	418	805	414	87
Avg.	0.468	0.495	0.683	0.711	0.671	0.699	-0.027	80	97	180	107	26

[†] and [‡] denote the runtime of our complete global routing flow and our proposed GAP-LA, respectively.

TABLE III
COMPARISON OF FOUR METRICS WITH TOP-3 WINNERS IN THE ISPD 2025 CONTEST.

Case	WNS				TNS				Power				Congestion			
	1st	2nd	3rd	Ours	1st	2nd	3rd	Ours	1st	2nd	3rd	Ours	1st	2nd	3rd	Ours
1	-0.432	-0.398	-0.381	-0.365	-1325.8	-1340.2	-1138.4	-997.9	0.646092	0.646078	0.646080	0.646076	5846461	5902619	8003814	6662339
2	-0.420	-0.424	-0.407	0.388	-10366.2	-10774.9	-9344.3	-9602.9	3.05441	3.05301	3.05345	3.05349	21332547	20468992	25412296	22947622
3	-56.919	-55.841	-55.914	-56.253	-521344.6	-514660.3	-514674.3	-515014.3	2.94054	2.94011	2.93806	2.93766	13315606	13686714	15687876	13562374
4	-0.379	-0.489	-0.520	-0.387	-1610.0	-2225.5	-2524.3	-1711.6	0.14310	0.14515	0.14522	0.14383	3019425	2478318	3469019	2689765
5	-0.305	-0.347	-0.275	-0.327	-20473.8	-21709.1	-19338.7	-17619.7	7.69208	7.73386	7.55296	7.59214	55005746	49071540	97506553	67934233
6	-0.266	-0.315	-0.276	-0.247	-59712.5	-62460.0	-59533.5	-52800.0	23.4497	23.5781	23.2200	23.1486	236920427	192012708	289712328	24407995
7	-1.756	-0.737	-0.633	-0.645	-650.1	-149.5	-162.4	-111.5	0.15614	0.15613	0.15611	0.15614	4349151	4651055	4386728	4371048
8	-3.984	0.000	-2.747	0.000	-2859.8	0.000	-2936.0	0.000	0.30473	0.30477	0.30478	0.30481	22567636	21307154	20564539	22506663
9	0.000	0.000	0.000	0.000	0.000	0.000	0.000	0.000	0.13625	0.13626	0.13628	0.13629	14061155	16352692	13637302	13242873
10	-0.342	-0.472	-0.440	0.353	-1356.1	-1920.7	-1806.8	-1312.2	0.14303	0.14485	0.14520	0.14390	2232008	2122543	2168599	2087873
11	-0.433	-0.460	-0.373	-0.404	-32016.1	-34846.1	-26801.4	-27116.0	8.36880	8.35859	7.94192	8.19256	52783071	49722314	132027917	68117588
12	-0.223	-0.294	-0.200	-0.199	-42564.1	-50372.4	-39516.2	-38106.6	24.2439	24.3801	23.9679	24.0595	242737068	214110807	335020596	232170935
Avg.	-5.455	-4.981	-5.181	-4.964	-57856.6	-58371.6	-56481.4	-53366.1	5.93989	5.96475	5.85066	5.87625	56180858	49323955	78966464	58391776
Ratio	1.099	1.003	1.044	1.000	1.045	1.054	1.020	1.000	1.011	1.015	0.996	1.000	0.962	0.845	1.352	1.000

B. Ablation Studies

To evaluate the effectiveness of our proposed strategies, we compare the WNS and TNS result of our solution on each design with those that do not use these strategies. Table IV shows that our framework achieves better WNS results in 11 of the 12 ISPD2025 benchmark cases and better TNS results in all 12 cases. The net ordering and batching strategy enables more precise optimization of critical nets, significantly outperforming the naive strategy that ignores timing analysis information. This advantage is particularly evident in cases sensitive to critical net delay and capacitance, such as case 9. The look-ahead strategy also proves crucial in certain cases, including case 4.

Table V presents the number of critical paths and nets for several selected cases. The results show that only a small fraction of nets (less than 1% of all nets) in the netlist play a significant role in timing closure. In case 8, focusing optimization efforts on the 9 critical nets with high timing cost weights is sufficient to achieve zero slack, demonstrating the effectiveness of our critical net selection strategy.

Figure 11 illustrates the variations in overflow, WNS, and TNS as the delay and capacitance weights increase. Our framework generates solutions with improved timing performance but higher congestion, indicating that the method can adapt to different optimization priorities to meet diverse design requirements.

TABLE IV
ABLATION STUDY ON OUR CRITICAL NET ANALYSIS-BASED NET ORDERING AND BATCHING STRATEGY AND LOOK AHEAD STRATEGY.

Case		1	2	3	4	5	6	7	8	9	10	11	12	Avg.
WNS	Ours	-0.365	-0.388	-56.25	-0.387	-0.327	-0.247	-0.645	0.000	0.000	-0.353	-0.404	-0.199	-4.961
	w/o ordering	-0.385	-0.404	-60.415	-0.488	-0.293	-0.272	-1.458	0.000	-10.501	-0.413	-0.430	-0.214	-6.273
	w/o ahead	-0.368	-0.398	-56.316	-0.426	-0.330	-0.251	-0.791	0.000	0.000	-0.361	-0.405	-0.198	-4.987
TNS	Ours	-997.9	9602.9	-515014.3	-1711.6	-17619.7	-52800.0	-111.5	0.000	0.000	-1312.2	-27116.0	-38106.6	-55366.1
	w/o ordering	-1065.1	-9768.3	-549035.6	-2167.1	-18133.0	-56966.8	-387.3	0.000	-10903.8	-1626.9	-28959.3	-39449.7	-59874.4
	w/o ahead	-1061.4	-10036.4	-515775.7	-1839.4	-18161.2	-53875.2	-194.1	0.000	0.000	-1382.5	-27565.8	-38441.1	-55694.4

TABLE V
NUMBER OF CRITICAL PATHS AND CRITICAL NETS ON SEVERAL SELECTED CASES.

Case	# Crit. Paths	# Crit. Nets	N_{net}	Crit. Ratio
1	1585	360	123900	0.291%
2	1098	458	736883	0.062%
3	4102	810	136120	0.595%
7	312	91	105924	0.086%
8	630	9	768239	0.001%
9	4034	816	135814	0.601%

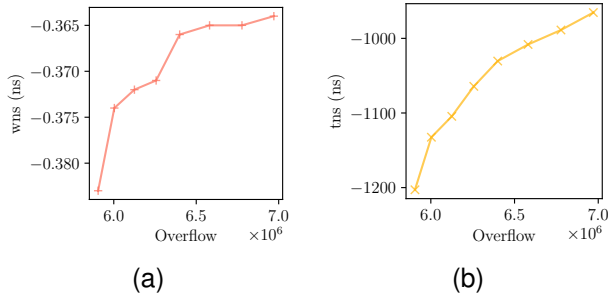


Fig. 11. Overflow, (a) WNS and (b) TNS in case 1 under different delay and capacitance weights.

V. CONCLUSION

In this paper, we present a GPU-accelerated performance-driven layer assignment framework that generates high-quality routing solutions from 2D routing results. The framework integrates a static timing analysis engine to schedule optimal net ordering and task batching for effective performance optimization. To address the delay cost optimization of large-scale designs with up to 10 million nets, we design GPU kernels for layer assignment using a look-ahead strategy. Compared with the top-3 winners of the contest, our router achieves 0.3%–9.9% better WNS and 2.0%–5.4% better TNS with acceptable runtime overhead.

REFERENCES

- [1] T.-H. Lee and T.-C. Wang, "Congestion-constrained layer assignment for via minimization in global routing," *IEEE Transactions on Computer-Aided Design of Integrated Circuits and Systems*, vol. 27, no. 9, pp. 1643–1656, 2008.
- [2] —, "Robust layer assignment for via optimization in multi-layer global routing," in *Proceedings of the 2009 International Symposium on Physical Design*, ser. ISPD '09. New York, NY, USA: Association for Computing Machinery, 2009, p. 159–166. [Online]. Available: <https://doi.org/10.1145/1514932.1514968>
- [3] C.-H. Hsu, H.-Y. Chen, and Y.-W. Chang, "Multi-layer global routing considering via and wire capacities," in *2008 IEEE/ACM International Conference on Computer-Aided Design*, 2008, pp. 350–355.

- [4] Y. Xu, Y. Zhang, and C. Chu, "Fastroute 4.0: Global router with efficient via minimization," in *2009 Asia and South Pacific Design Automation Conference*, 2009, pp. 576–581.
- [5] W.-H. Liu and Y.-L. Li, "Negotiation-based layer assignment for via count and via overflow minimization," in *16th Asia and South Pacific Design Automation Conference (ASP-DAC 2011)*, 2011, pp. 539–544.
- [6] K.-R. Dai, W.-H. Liu, and Y.-L. Li, "Nctu-gr: Efficient simulated evolution-based rerouting and congestion-relaxed layer assignment on 3-d global routing," *IEEE Transactions on Very Large Scale Integration (VLSI) Systems*, vol. 20, no. 3, pp. 459–472, 2012.
- [7] Y.-J. Jiang and S.-Y. Fang, "Coala: Concurrently assigning wire segments to layers for 2-d global routing," *IEEE Transactions on Computer-Aided Design of Integrated Circuits and Systems*, vol. 42, no. 2, pp. 569–582, 2023.
- [8] J. Liu, C.-W. Pui, F. Wang, and E. F. Y. Young, "Cugr: Detailed-routability-driven 3d global routing with probabilistic resource model," in *2020 57th ACM/IEEE Design Automation Conference (DAC)*, 2020, pp. 1–6.
- [9] S. Lin and M. D. F. Wong, "Superfast full-scale cpu-accelerated global routing," in *Proceedings of the 41st IEEE/ACM International Conference on Computer-Aided Design*, ser. ICCAD '22. New York, NY, USA: Association for Computing Machinery, 2022. [Online]. Available: <https://doi.org/10.1145/3508352.3549474>
- [10] S. Lin, J. Liu, E. F. Y. Young, and M. D. F. Wong, "Gamer: Gpu-accelerated maze routing," *IEEE Transactions on Computer-Aided Design of Integrated Circuits and Systems*, vol. 42, no. 2, pp. 583–593, 2023.
- [11] J. Liu and E. F. Young, "Edge: Efficient dag-based global routing engine," in *2023 60th ACM/IEEE Design Automation Conference (DAC)*, 2023, pp. 1–6.
- [12] B. Yu, D. Liu, S. Chowdhury, and D. Z. Pan, "Tila: Timing-driven incremental layer assignment," in *2015 IEEE/ACM International Conference on Computer-Aided Design (ICCAD)*, 2015, pp. 110–117.
- [13] D. Liu, B. Yu, S. Chowdhury, and D. Z. Pan, "Incremental layer assignment for critical path timing," in *2016 53rd ACM/EDAC/IEEE Design Automation Conference (DAC)*, 2016, pp. 1–6.
- [14] S.-Y. Han, W.-H. Liu, R. Ewetz, C.-K. Koh, K.-Y. Chao, and T.-C. Wang, "Delay-driven layer assignment for advanced technology nodes," in *2017 22nd Asia and South Pacific Design Automation Conference (ASP-DAC)*, 2017, pp. 456–462.
- [15] X. Zhang, Z. Zhuang, G. Liu, X. Huang, W.-H. Liu, W. Guo, and T.-C. Wang, "Minidelay: Multi-strategy timing-aware layer assignment for advanced technology nodes," in *2020 Design, Automation & Test in Europe Conference & Exhibition (DATE)*, 2020, pp. 586–591.
- [16] L. Jiang, Z. Li, C. Bao, G. Liu, X. Huang, W.-H. Liu, and T.-C. Wang, "La-svr: A high-performance layer assignment algorithm with slew violations reduction," in *2022 IFIP/IEEE 30th International Conference on Very Large Scale Integration (VLSI-SoC)*, 2022, pp. 1–6.
- [17] Y. Lin, Z. Jiang, J. Gu, W. Li, S. Dhar, H. Ren, B. Khailany, and D. Z. Pan, "Dreamplace: Deep learning toolkit-enabled gpu acceleration for modern vlsi placement," *IEEE Transactions on Computer-Aided Design of Integrated Circuits and Systems*, vol. 40, no. 4, pp. 748–761, 2021.
- [18] Y. Lin, D. Z. Pan, H. Ren, and B. Khailany, "Dreamplace 2.0: Open-source gpu-accelerated global and detailed placement for large-scale vlsi designs," in *2020 China Semiconductor Technology International Conference (CSTIC)*, 2020, pp. 1–4.
- [19] J. Gu, Z. Jiang, Y. Lin, and D. Z. Pan, "Dreamplace 3.0: Multi-electrostatics based robust vlsi placement with region constraints," in *2020 IEEE/ACM International Conference On Computer Aided Design (ICCAD)*, 2020, pp. 1–9.
- [20] P. Liao, S. Liu, Z. Chen, W. Lv, Y. Lin, and B. Yu, "Dreamplace 4.0: Timing-driven global placement with momentum-based net weighting," in *2022 Design, Automation & Test in Europe Conference & Exhibition (DATE)*, 2022, pp. 939–944.

- [21] L. Liu, B. Fu, M. D. F. Wong, and E. F. Y. Young, “Xplace: an extremely fast and extensible global placement framework,” in *Proceedings of the 59th ACM/IEEE Design Automation Conference*, ser. DAC '22. New York, NY, USA: Association for Computing Machinery, 2022, p. 1309–1314. [Online]. Available: <https://doi.org/10.1145/3489517.3530485>
- [22] J. Mai, C. Zhao, Z. Zhang, Z. Di, Y. Lin, R. Wang, and R. Huang, “Legalm: Efficient legalization for mixed-cell-height circuits with linearized augmented lagrangian method,” in *Proceedings of the 2025 International Symposium on Physical Design*, ser. ISPD '25. New York, NY, USA: Association for Computing Machinery, 2025, p. 22–30. [Online]. Available: <https://doi.org/10.1145/3698364.3705356>
- [23] S. Liu, P. Liao, R. Zhang, Z. Chen, W. Lv, Y. Lin, and B. Yu, “Fastgr: Global routing on cpu-gpu with heterogeneous task graph scheduler,” in *2022 Design, Automation & Test in Europe Conference & Exhibition (DATE)*, 2022, pp. 760–765.
- [24] S. Lin, L. Xiao, J. Liu, and E. F. Y. Young, “Instantgr: Scalable gpu parallelization for global routing,” in *Proceedings of the 43rd IEEE/ACM International Conference on Computer-Aided Design*, ser. ICCAD '24. New York, NY, USA: Association for Computing Machinery, 2025. [Online]. Available: <https://doi.org/10.1145/3676536.3676787>
- [25] C. Zhao, Z. Guo, R. Wang, Z. Wen, Y. Liang, and Y. Lin, “Helem-gr: Heterogeneous global routing with linearized exponential multiplier method,” in *Proceedings of the 43rd IEEE/ACM International Conference on Computer-Aided Design*, ser. ICCAD '24. New York, NY, USA: Association for Computing Machinery, 2025. [Online]. Available: <https://doi.org/10.1145/3676536.3676650>
- [26] R. Liang, A. Agnesina, W.-H. Liu, M. Liberty, H.-T. Chang, and H. Ren, “Invited: Ispd 2025 performance-driven large scale global routing contest,” in *Proceedings of the 2025 International Symposium on Physical Design*, ser. ISPD '25. New York, NY, USA: Association for Computing Machinery, 2025, p. 252–256. [Online]. Available: <https://doi.org/10.1145/3698364.3715706>
- [27] W. C. Elmore, “The transient response of damped linear networks with particular regard to wideband amplifiers,” *Journal of Applied Physics*, vol. 19, no. 1, pp. 55–63, 01 1948. [Online]. Available: <https://doi.org/10.1063/1.1697872>
- [28] T. Ajayi, D. Blaauw, T.-B. Chan, C.-K. Cheng, V. A. Chhabria, D. K. Choo, M. Coltella, R. G. Dreslinski, M. Fogac,a, S. M. Hashemi, A. A. Ibrahim, A. B. Kahng, M. Kim, J. Li, Z. Liang, U. Mallappa, P. I. Pénczes, G. Pradipta, S. Reda, A. Rovinski, K. Samadi, S. S. Sapatnekar, L. K. Saul, C. Sechen, V. Srinivas, W. Swartz, D. Sylvester, D. Urquhart, L. Wang, M. Woo, and B. Xu, “Openroad: Toward a self-driving, open-source digital layout implementation tool chain,” 2019. [Online]. Available: <https://api.semanticscholar.org/CorpusID:210937106>
- [29] Z. Guo, T.-W. Huang, and Y. Lin, “Accelerating static timing analysis using cpu-gpu heterogeneous parallelism,” *IEEE Transactions on Computer-Aided Design of Integrated Circuits and Systems*, pp. 1–1, 2023.
- [30] Z. Guo, Z. Zhang, W. Li, T.-W. Huang, X. Shi, Y. Du, Y. Lin, R. Wang, and R. Huang, “Heteroexcept: A cpu-gpu heterogeneous algorithm to accelerate exception-aware static timing analysis,” in *2024 IEEE/ACM International Conference on Computer-Aided Design (ICCAD)*. ACM, 2024.
- [31] “Heterosta.” [Online]. Available: <https://heterosta.pkueda.org/cn/>